Pergamon

Polyhedron Vol. 14, No. 15–16, pp. 2215–2220, 1995

0277-5387/95 $9.50+0.00

0277-5387(94)00499-4

SYNTHESIS AND CHARACTERIZATION OF TWO NEW MOLYBDENUM(0) σ-ARYL COMPLEXES OF THE TYPE $[N(PPh_3)_2][Mo(C_6F_5)L(CO)_2\{P(OMe)_3\}_2]$: X-RAY CRYSTAL STRUCTURE OF BIS(TRIPHENYLPHOSPHINE)IMINIUM PENTAFLUOROPHENYL(*mer*-TRICARBONYL) *trans*-BIS(TRIMETHYLPHOSPHITE)MOLYBDATE(0)

D. F. MULLICA,* S. L. GIPSON,* M. SU and E. L. SAPPENFIELD

Department of Chemistry, Baylor University, Waco, TX 76798, U.S.A.

(*Received* 1 *November* 1994; *accepted* 25 *November* 1994)

Abstract—The complex $[cis\text{-}mer\text{-}Mo(C_6F_5)(CO)_2\{P(OMe)_3\}_3]^-$ reacts with the π-acid ligands CO and ^{t}BuNC to yield the substitution products $[Mo(C_6F_5)L(CO)_2\{P(OMe)_3\}_2]^-$, both isolated as the $N(PPh_3)_2^+$ salts. Both new complexes have been fully characterized by IR, ^{1}H and ^{31}P NMR, and elemental analysis. The electrochemistry of all three complexes has also been examined. The structure of $[N(PPh_3)_2][mer\text{-}trans\text{-}Mo(C_6F_5)(CO)_3\{P(OMe)_3\}_2]$ has been determined by X-ray crystallography. The compound displays essentially octahedral geometry about the molybdenum atom. Averaged important bond distances and angles are: Mo—C(O) = 1.99(3); C≡O = 1.18(1); Mo—P = 2.418(1); P—O(C) = 1.614(9); O—C = 1.440(11); N—P = 1.578(9); P—C(ring) = 1.805(4) Å; and Mo—P—O = 119(4)°; P—O—C = 120.9(7)°; N—P—C(ring) = 111(2)°.

We have been investigating the synthesis and redox reactivity of novel molybdenum(0) σ-pentafluorophenyl complexes accessible through the reduction of $[Mo(C_6F_5)(CO)_2(\eta\text{-}C_7H_7)]$.[1] Until our work, the only reported molybdenum(0) complexes containing organic σ-bound-carbon ligands were the heptafluoro-1-methylpropenyl complex, $[Mo(CO)_5(C_4F_7)]^{-2}$ and the acetylenide complexes $[Mo(C{\equiv}CR)(CO)_4L]^-$ (L = CO or PPh_3; R = Me or Ph).[3] Upon attempting to study the electrochemistry of $[cis\text{-}mer\text{-}Mo(C_6F_5)(CO)_2\{P(OMe)_3\}_3]^-(\mathbf{1}^-)$ under an atmosphere of CO, we found that it underwent a rapid substitution reaction even in the absence of electron transfer. Complex $\mathbf{1}^-$ undergoes a similar reaction with another π-acid ligand, ^{t}BuNC. We now wish to report the details of the synthesis and characterization of the resulting two new molybdenum(0) σ-aryl complexes, $[Mo(C_6F_5)L(CO)_2\{P(OMe)_3\}_2]^-$ (L = CO or ^{t}BuNC), both isolated as the $N(PPh_3)_2^+$ salts. In addition, the X-ray crystal structure of the tricarbonyl complex $[N(PPh_3)_2][mer\text{-}trans\text{-}Mo(C_6F_5)(CO)_3\{P(OMe)_3\}_2]$ has been determined.

EXPERIMENTAL

The complex $Na[cis\text{-}mer\text{-}Mo(C_6F_5)(CO)_2\{P(OMe)_3\}_3]Na$ [1] was prepared by the published procedure.[1a] The Na^+ cation was replaced with $N(PPh_3)_2^+$ by exchange with $[N(PPh_3)_2]Cl$ in tetrahydrofuran (THF). All reactions were carried out under argon and all solvents were dried, distilled and deoxygenated before use. IR spectra were obtained using a Mattson Instruments Cygnus 100 FTIR and ^{1}H and ^{31}P-$\{^1H\}$ NMR spectra were obtained on a Bruker AMX 360 NMR spectrometer. Chemical shifts were assigned relative to TMS internal standard for ^{1}H or 85% H_3PO_4 external standard for ^{31}P. Cyclic voltammetry and controlled potential electrolyses were performed using a Bioanalytical Systems BAS 100A electrochemical analyser. Conventional cyclic voltammetry was done using a 0.5 mm Pt disc working electrode,

---

*Authors to whom correspondence should be addressed.

Pt wire auxiliary electrode, and Ag/AgCl reference electrode. Fast scan cyclic voltammetry used a BAS low current module and a 0.1 mm Pt disc working electrode. Controlled potential electrolyses were performed using 25×25 mm^2 platinum foil working and auxiliary electrodes and a silver wire quasi-reference electrode. All potentials are expressed relative to the formal potential of the ferrocenium–ferrocene couple, which we measure as approximately $+0.45$ V vs Ag/AgCl. Elemental analyses were performed by Texas Analytical Laboratories, Inc., Stafford, TX.

Preparation of $[N(PPh_3)_2]$[*mer-trans*-Mo$(C_6F_5)(CO)_3\{P(OMe)_3\}_2$] ($[N(PPh_3)_2]$[**2**])

Complex $[N(PPh_3)_2]$[**1**] (0.221 g, 0.180 mmol) was dissolved in CH_2Cl_2 (6 cm^3), and CO was bubbled through the solution for 40–60 min, during which time the solution volume decreased to 2–2.5 cm^3. The solution was then layered with hexane (15 cm^3) for 24 h. $[N(PPh_3)_2]$[**2**] precipitated as pale yellow crystals which were filtered, washed with hexane (3×3 cm^3), and then vacuum dried (0.165 g, 81%). Found: C, 53.3; H, 4.2; N, 1.6. $C_{51}H_{48}F_5MoNO_9P_4$ requires: C, 54.0; H 4.3; N, 1.2%. IR (CH_2Cl_2): ν_{max} (cm^{-1}) (CO) 1854 vs, 1798 s. NMR (CD_2Cl_2): δ_H 7.4–7.7 [m, $N(PPh_3)_2^+$], 3.39 [t, ^3J(PH)$+^5J$(PH) = 11.0 Hz, $P(OMe)_3$]; δ_P 183 [t, ^4J(FP) = 4 Hz, $P(OMe)_3$], 21 [s, $N(PPh_3)_2^+$].

Preparation of $[N(PPh_3)_2]$[*cis-trans*-Mo(C_6F_5)(^{t}BuNC)$(CO)_2\{P(OMe)_3\}_2$] ($[N(PPh_3)_2]$[**3**])

Complex $[N(PPh_3)_2]$[**1**] (0.221 g, 0.180 mmol) was dissolved in CH_2Cl_2 (2 cm^3) and mixed with CH_2Cl_2 (1 cm^3) containing ^{t}BuNC (0.1 cm^3, 0.88 mmol). The solution was then layered with hexane (15 cm^3) for 48 h. $[N(PPh_3)_2]$[3] precipitated as an orange oil which was washed with hexane (3×3 cm^3) and then vacuum dried to give a yellow solid (0.120 g, 56%). Found: C, 55.6; H, 5.0; N, 2.4. $C_{55}H_{57}F_5MoN_2O_8P_4$ requires: C, 55.6; H, 4.8, N, 2.4%. IR (CH_2Cl_2): ν_{max} (cm^{-1}) (CO) 1843 vs, 1756 s. NMR (CD_2Cl_2): δ_H 7.4–7.7 [m, $N(PPh_3)_2^+$], 3.39 [t, ^3J(PH)$+^5J$(PH) = 10.8 Hz, $P(OMe)_3$], 1.37 [s, ^{t}BuNC]; δ_P 185 [t, $P(OMe)_3$], 22 [s, $N(PPh_3)_2^+$].

Crystal structure of $[N(PPh_3)_2]$[*mer-trans*-Mo$(C_6F_5)(CO)_3\{P(OMe)_3\}_2$] ($[N(PPh_3)_2]$[**2**])

A clear yellow crystal ($0.28 \times 0.56 \times 0.56$ mm^3) of **2** was selected for X-ray diffraction analysis on the basis of optical purity. The homogeneity of the crystal was verified by a conoscopic examination which also confirmed the biaxial nature of the crystal. After attaching the studied crystal to a glass fibre and mounting it on an Enraf–Nonius CAD4-F automated diffractometer, the data were collected in the $\omega - 2\theta$ mode at a varied scan rate (0.56–5.17° min^{-1}) and in the 2θ range of 3.0–40.0° (h: 0–10, k: -13–13, l: -16–16). The orientation matrix used for data collection and the unit cell parameters (final lattice constants at high θ angles, $>20°$) were obtained from a least-squares refinement of 25 randomly selected and accurately centred reflections. The crystal stability and electronic hardware reliability were verified by monitoring three standard reflections as a function of time (every 2 h of exposure time, $<2.0\%$ dev.). A total of 4981 data points were measured of which 4663 were independent and 4363 with $F > 4.0\sigma(F)$ were included in the structural refinement ($R_{int} = 0.021$). All intensity data were corrected for Lorentz and polarization effects after which an empirical absorption correction based on high-angle ψ scans (min., max. transmission factors = 0.7869, 0.9993) was performed. Crystal data, experimental and statistical summaries, and pertinent refinement parameters are presented in Table 1.

The phase problem was solved by direct and Fourier methods. The direct method located the Mo, P and N atoms and approximately half of the O and C atoms in triclinic space group $P\bar{1}$ (No. 2). Difference Fourier mapping found all other non-hydrogen atoms. The data were tested using the program MISSYM[4] which revealed additional symmetry (centre of inversion). Also, an $N(Z)$ test[5] to the observed data provided further evidence that the data best fit the centrosymmetric $P\bar{1}$ space group. The hydrogen atoms were generated with idealized geometry and were constrained (at 0.96 Å) to ride on their connected atoms with fixed isotropic thermal factors, $U = 0.08$ Å^2. The model was refined by the full-matrix least-squares method[6] and after applying a secondary extinction correction [$g = 2.3\ (12) \times 10^{-4}$ e^{-2}], anisotropic refinement of all non-hydrogen atoms yielded final residual index values (Table 1). A final electron density map revealed a maximum peak of 0.68e$^-$ Å^{-3} and the deepest hole showed a density of -0.89e$^-$ Å^{-3}, both in the vicinity of the heavy metal atom. Elsewhere only a random fluctuating background was observed. The quantity minimized was $\Sigma w(|F_o| - |F_c|)^2$ and the weighting function $w = [\sigma^2(F) + 0.0053F^2]^{-1}$. Atomic scattering factors and anomalous dispersion factors were taken from the usual source.[7] Fractional atomic coordinates, thermal parameters and a list of structure factor values have been deposited as supplementary

Table 1. Data for crystal structure analysis of compound **2**

Molecular formula	$C_{51}H_{48}F_5MoNO_9P_4$
M_r	1133.8
Crystal system	Triclinic
Space group	$P\bar{1}$ (No. 2)
a (Å)	11.416(2)
b (Å)	13.839(3)
c (Å)	17.546(2)
α (°)	67.58(1)
β (°)	78.68(2)
γ (°)	85.08(2)
V (Å^3)	2515.3(8)
Z	2
D_c (Mg m^{-3})	1.498
F(000)	1160
Radiation (λ_{mean} Å^{-1})	Mo-$K_{\bar{\alpha}}$ (0.71073)
μ (Mo-K_α) (mm^{-1})	0.452
T (K)	173
$\Delta\theta$ range (°)	1.5 to 20.0
Unique reflections	4363
R_{int}	0.0266
Refined parameters	641
Data-to-parameter ratio	6.8 : 1
R (R_{all}) $= \Sigma \lVert F_o\rvert - \lvert F_o \rVert / \Sigma \lvert F_o \rvert$	0.042(0.046)
$R_w = \Sigma\sqrt{w} \lVert F_o\rvert - \lvert F_o\rVert / \Sigma\sqrt{w}\, \lvert F_o\rvert$	0.054
Residual density (max., min.) (e Å^{-3})	0.68, −0.80
Gnft (Σ_2)	1.05

material with the Editor, from whom copies are available upon request.

RESULTS AND DISCUSSION

Cyclic voltammetry of $[N(PPh_3)_2][\mathbf{1}]$ in THF displays an anodic peak at −0.78 V vs F^+c/Fc and a cathodic peak at −1.16 V on the return scan at a scan rate of 20 V s^{-1}. After the first scan, an additional anodic peak appears at −1.02 V. This behaviour is interpreted as indicative of a typical EC square scheme of coupled electron transfer and structure change, most probably a *cis/trans* or *mer/fac* isomerization.[8] The initial oxidation of $\mathbf{1}^-$ is followed by a rapid structural change to give a product which is reduced at −1.16 V. After the reduction, a slower structural change reforms $\mathbf{1}^-$. At high scan rates, oxidation of both forms of the anion are observed on the second scan, while at slower scan rates only the original anodic peak of $\mathbf{1}^-$ is observed on all scans. Controlled potential oxidation of a 7.5 mM solution of Na[**1**] in THF at 0.00 V vs F^+c/Fc consumed 1.4 F mol^{-1}, suggesting that the product is a neutral 17e$^-$ complex. The resulting solution showed a cyclic voltammogram almost identical to that of the starting material but with the open circuit potential shifted to more positive values. However, the oxidation product was not stable enough to be isolated from solution. The slow decomposition of the 17e$^-$ complex probably also explains the excess charge consumed in the electrolysis. Similar results were obtained with chemical oxidants.

Synthesis and characterization of $[N(PPh_3)_2]$[*mer-trans*-$Mo(C_6F_5)(CO)_3\{P(OMe)_3\}_2$] ($[N(PPh_3)_2][\mathbf{2}]$)

An attempt was made to study the cyclic voltammetry of complex $\mathbf{1}^-$ under an atmosphere of CO. However, it was found that when CO was passed through solutions of $[N(PPh_3)_2][\mathbf{1}]$, within 10 min the anodic and cathodic peaks of $\mathbf{1}^-$ disappeared. They were replaced by a similar couple with an anodic peak potential of −0.70 V vs F^+c/Fc and a cathodic peak potential of −0.80 V. Controlled potential oxidation resulted in rapid decomposition.

The reaction of $[N(PPh_3)_2][\mathbf{1}]$ with CO was then carried out on a preparative scale and the product was isolated. The IR spectrum of the product displayed two carbonyl stretching bands at 1854 and 1798 cm^{-1} (*cf* 1855 and 1758 cm^{-1} for $[N(PPh_3)_2][\mathbf{1}]$). The ^{1}H NMR spectrum of the product displayed an apparent triplet at 3.39 ppm (*cf*

3.43t + 3.51d for Na[**1**]) in addition to a multiplet from the $N(PPh_3)_2^+$ at 7.4–7.7 ppm. The ^{31}P-$\{^1H\}$ NMR spectrum showed a poorly resolved triplet at 183 ppm (*cf* 169tt + 179dt for Na[**1**]) in addition to the $N(PPh_3)_2^+$ resonance at 21 ppm. This spectroscopic evidence led to the conclusion that the $P(OMe)_3$ ligand *trans* to CO in complex **1**$^-$ had been replaced by CO to give complex **2**$^-$ with the formula [*mer-trans*-$Mo(C_6F_5)(CO)_3\{P(OMe)_3\}_2]^-$. Note that the apparent triplet observed in the ^1H NMR spectrum is typical of $X_nAA'X'_n$ systems[9] and is diagnostic of a mutually *trans* orientation for phosphine or phosphite ligands containing methyl groups.[10] Also note that the splitting of the ^{31}P NMR resonance of the phosphites is due to coupling with the two *ortho* fluorines of the pentafluorophenyl group.[1a] The identity of **2**$^-$ was confirmed by an X-ray crystal structure of $[N(PPh_3)_2]$[**2**] (see below).

Synthesis and characterization of $[N(PPh_3)_2]$[*cis-trans*-$Mo(C_6F_5)(^tBuNC)(CO)_2\{P(OMe)_3\}_2]$ ($[N(PPh_3)_2]$[**3**])

In order to explore the generality of the substitution reactions of complex **1**$^-$, reactions were attempted with several other potential ligands. No reaction occurred upon adding pyridine to a solution of **1**$^-$ in CH_2Cl_2, while an as yet uncharacterized product formed with 4-acetylpyridine. A clean substitution reaction did occur with tert-butylisocyanide. The product displayed carbonyl stretching bands at 1843 and 1756 cm^{-1}, ^1H NMR resonances at 3.39t and 1.55s ppm, and an unresolved triplet at 185 ppm in the ^{31}P-$\{^1H\}$ NMR spectrum (in addition to the $N(PPh_3)_2^+$ resonances). These spectroscopic data, as well as the elemental analysis, are in agreement with the assignment [*cis-trans*-$Mo(C_6F_5)(^tBuNC)(CO)_2\{P(OMe)_3\}_2]^-$ for the structure of **3**$^-$. The electrochemistry of complex **3**$^-$ is not as clean as that of **1**$^-$ and **2**$^-$. It displays an anodic peak at −0.88 V vs F^+c/Fc coupled to two cathodic peaks at −1.00 and −1.25 V.

Structure of $[N(PPh_3)_2]$[*mer-trans*-$Mo(C_6F_5)(CO)_3\{P(OMe)_3\}_2]$ ($[N(PPh_3)_2]$[**2**])

Compound **2** crystallizes in the triclinic space group $P\bar{1}$ and contains two molecules per unit cell. The zerovalent molybdenum atom is six-coordinated having a slightly distorted octahedral

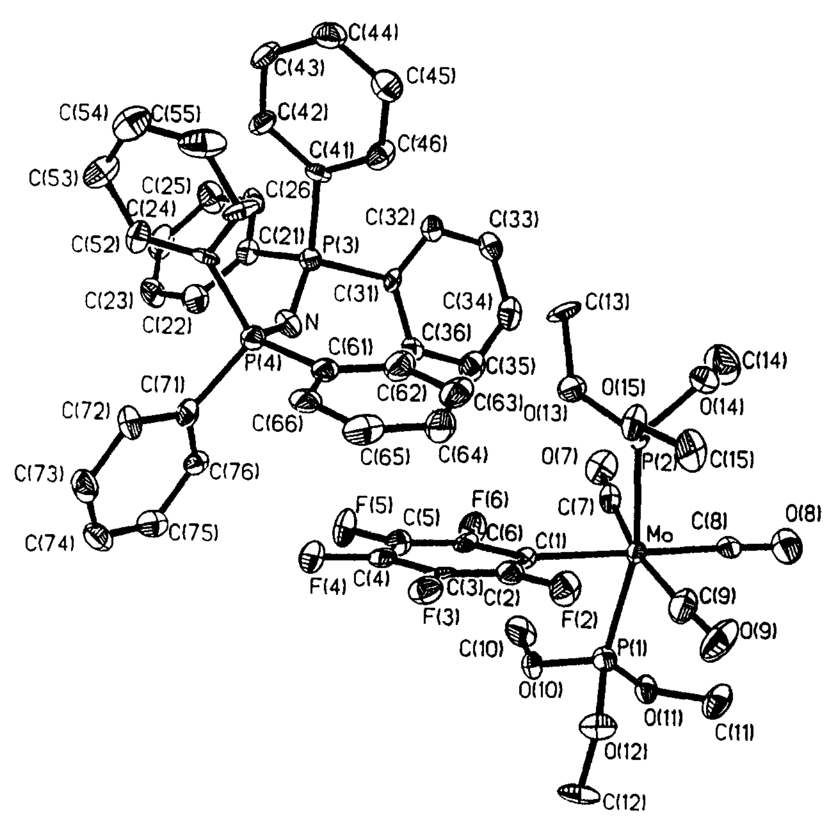

Fig. 1. Molecular structure of $[N(PPh_3)_2]$[*mer-trans*-$Mo(C_6F_5)(CO)_3\{P(OMe)_3\}_2$][**2**], showing the crystallographic number scheme.

geometry (Table 2). Molybdenum is bonded to two trimethylphosphite groups (*trans*), three carbonyl groups, and a pentafluorophenyl group. Figure 1 illustrates the molecular structure and the atom labelling scheme. The average ligand—Mo—ligand bond angle is 90(5)° although it is apparent that distortions occur within individual angles. The mean Mo—P and Mo—C(O) bond distances are 2.418(1) and 1.99(3) Å, respectively, which are consistent with experimental values found in the Cambridge Structure Database[11] and BIDICS.[12] The mean carbonyl bond length (C≡O) is 1.18(1) Å and Mo—C≡O bond angles range from 172.7 to 176.4°. This near linear arrangement is attributed to strong directional bonding related to the interaction of Mo 4*d* orbitals and the CO orbitals. The pentafluorophenyl group is planar having an average deviation from planarity of 0.006 Å. The C—F bond distances are normal [mean, 1.55(9) Å] and the F atoms are in plane with the C(1)—C(6) ring. The plane associated with the Mo, C(1), C(7), C(8) and C(9) atoms was also tested for planarity (standard deviation, 0.019 Å). There is a dihedral angle of 17.4° between this plane and the plane of the

Table 2. Selected bond lengths (Å) and angles (°)

Mo—C(1)	2.324(5)	P(1)—O(10)	1.617(3)
Mo—P(1)	2.417(1)	P(1)—O(11)	1.617(3)
Mo—P(2)	2.419(1)	P(1)—O(12)	1.611(3)
Mo—C(7)	2.017(4)	P(2)—O(13)	1.611(3)
Mo—C(8)	1.937(5)	P(2)—O(14)	1.629(4)
Mo—C(9)	2.001(4)	P(2)—O(15)	1.600(2)
C(7)—O(7)	1.159(5)	O(10)—C(10)	1.424(4)
C(8)—O(8)	1.188(6)	O(11)—C(11)	1.449(6)
C(9)—O(9)	1.181(5)	O(12)—C(12)	1.456(5)
N—P(3)	1.586(4)	O(13)—C(13)	1.442(5)
N—P(4)	1.569(3)	O(14)—C(14)	1.428(5)
P(3)—C(21)	1.810(4)	O(15)—C(15)	1.442(5)
P(3)—C(31)	1.810(4)	C(2)—F(2)	1.361(4)
P(3)—C(41)	1.799(4)	C(3)—F(3)	1.342(4)
P(4)—C(51)	1.804(3)	C(4)—F(4)	1.346(5)
P(4)—C(61)	1.807(4)	C(5)—F(5)	1.362(4)
P(4)—C(71)	1.801(5)	C(6)—F(6)	1.364(4)
C(1)—Mo—P(1)	84.8(1)	Mo—P(1)—O(10)	119.8(1)
C(1)—Mo—P(2)	82.2(1)	Mo—P(1)—O(11)	122.5(1)
C(1)—Mo—C(7)	97.6(2)	Mo—P(1)—O(12)	114.3(1)
C(1)—Mo—C(8)	175.6(1)	Mo—P(2)—O(13)	111.2(1)
C(1)—Mo—C(9)	93.3(2)	Mo—P(2)—O(14)	121.4(1)
P(1)—Mo—P(2)	166.3(1)	Mo—P(2)—O(15)	122.7(1)
P(3)—N—P(4)	139.4(2)	P(1)—O(10)—C(10)	121.3(3)
N—P(3)—C(21)	110.5(2)	P(1)—O(11)—C(11)	120.4(2)
N—P(3)—C(31)	108.3(2)	P(1)—O(12)—C(12)	121.0(2)
N—P(3)—C(41)	114.4(2)	P(2)—O(13)—C(13)	121.6(3)
N—P(4)—C(51)	115.2(2)	P(2)—O(14)—C(14)	119.5(3)
N—P(4)—C(61)	110.8(2)	P(2)—O(15)—C(15)	121.5(2)
N—P(4)—C(71)	109.7(2)		

	Distances		Angles	
Ring	Mean	Range	Mean	Range
C(1)–C(6)	1.382(12)	1.362–1.401	120(4)	112.4–125.4
C(21)–C(26)	1.382(5)	1.376–1.391	120.0(5)	119.5–120.8
C(31)–C(36)	1.391(12)	1.368–1.406	120.0(3)	119.4–120.4
C(41)–C(46)	1.383(7)	1.370–1.391	120.0(8)	118.8–121.3
C(51)–C(56)	1.383(13)	1.363–1.399	120.0(11)	118.0–121.4
C(61)–C(66)	1.381(7)	1.371–1.389	120.0(5)	119.2–120.6
C(71)–C(76)	1.386(13)	1.365–1.400	120.0(6)	119.0–120.7

pentafluorophenyl ring. The respective average P—O and O—CH_3 distances of 1.614(9) and 1.440(11) Å are in agreement with published values[11,12] as are the mean N—P [1.578(9) Å] and P—C(ring) [1.805(4) Å] bond lengths. The planarity of each phenyl ring was verified using the program PLANES[13] which produced an average deviation from planarity for the six phenyl rings of 0.006(2) Å. Details related to the N—P—C angles and the mean C—C distances and C—C—C angles of each phenyl ring are presented in Table 2.

Acknowledgement—We thank the Robert A. Welch Foundation (Grant No. AA-0668 and No. AA-1083) and Baylor University, in part, for support of this research.

REFERENCES

1. (a) S. L. Gipson, D. F. Mullica, E. L. Sappenfield, M. L. Hander and D. H. Leschnitzer, *J. Chem. Soc., Dalton Trans.* 1992, 521; (b) M. Su, S. L. Gipson, D. F. Mullica, E. L. Sappenfield and D. H. Leschnitzer, *J. Chem. Soc., Dalton Trans.* 1993, 3323.
2. W. J. Schlientz and J. K. Ruff, *J. Organomet. Chem.* 1971, **33**, C64.
3. W. J. Schlientz and J. K. Ruff, *J. Chem. Soc.* (*A*) 1971, 1139.
4. E. J. Gabe, Y. Le Page, J.-P. Charland and F. L. Lee, *J. Appl. Cryst.* 1989, **22**, 384.
5. E. R. Howells, D. C. Phillips and D. Rogers, *Acta Cryst.* 1959, **3**, 210.
6. SHELXTL-PC. Siemens Analytical X-ray Instruments, Madison, WI (1989).
7. J. A. Ibers and W. C. Hamilton, *International Tables for X-ray Crystallography*, Vol. IV. Kynoch Press, Birmingham (1974).
8. W. E. Geiger, *Prog. Inorg. Chem.* 1985, **33**, 275 and references therein.
9. (a) R. D. Bertrand, F. B. Ogilvie and J. G. Verkade, *J. Am. Chem. Soc.* 1970, **92**, 1908; (b) R. K. Harris, *Can. J. Chem.* 1964, **42**, 2275.
10. R. V. Parish, *NMR, NQR, EPR, and Mössbauer Spectroscopy in Inorganic Chemistry*, p. 47. Ellis Horwood, New York (1990).
11. A. G. Orpen, L. Brammer, F. H. Allen, O. Kennard, D. G. Watson and R. Taylor, *J. Chem. Soc., Dalton Trans.* 1989, **S1**.
12. *Bond Index of the Determination of Inorganic Crystal Structure*. Institute for Material Research, Hamilton, Canada (1969–1981).
13. V. Shoemaker, J. Waser, R. E. Marsh and G. Bergman, *Acta Cryst.* 1959, **12**, 600.